DOI: 10.1002/asia.200700173

Highly Ordered Mesoporous Carbonaceous Frameworks from a Template of a Mixed Amphiphilic Triblock-Copolymer System of PEO–PPO–PEO and Reverse PPO–PEO–PPO

Yan Huang,[a] Huaqiang Cai,[a] Ting Yu,[a] Xiuli Sun,[b] Bo Tu,[a] and Dongyuan Zhao*[a]

Abstract: A series of highly ordered mesoporous carbonaceous frameworks with diverse symmetries have been successfully synthesized by using phenolic resols as a carbon precursor and mixed amphiphilic surfactants of poly(ethylene oxide)-*b*-poly(propylene oxide)-*b*-poly(ethylene oxide) (PEO–PPO–PEO) and reverse PPO–PEO–PPO as templates by the strategy of evaporation-induced organic–organic self-assembly (EISA). The transformation of the ordered mesostructures from face-centered ($Fd\bar{3}m$) to body-centered cubic ($Im\bar{3}m$), then 2D hexagonal ($P6mm$), and eventually to cubic bicontinuous ($Ia\bar{3}d$) symmetry has been achieved by simply adjusting the ratio of triblock copolymers to resol precursor and the relative content of PEO–PPO–PEO copolymer F127, as confirmed by small-angle X-ray scattering (SAXS), transmission electron microscopy (TEM), and nitrogen-sorption measurements. The blends of block copolymers can interact with resol precursors and tend to self-assemble into cross-linking micellar structures during the solvent-evaporation process, which provides a suitable template for the construction of mesostructures. The assembly force comes from the hydrogen-bonding interactions between organic mixed micelles and the resol-precursor matrix. The BET surface area for the mesoporous carbonaceous samples calcined at 600 °C under nitrogen atmosphere is around 600 $m^2 g^{-1}$, and the pore size can be adjusted from 2.8 to 5.4 nm. An understanding of the organic–organic self-assembly behavior in the mixed amphiphilic surfactant system would pave the way for the synthesis of mesoporous materials with controllable structures.

Keywords: amphiphiles · block copolymers · mesophases · mesoporous materials · self-assembly

Introduction

Ordered mesoporous carbonaceous materials have attracted tremendous attention owing to their potential applications in many areas of materials science, such as catalysis,[1] sensors,[2] bioreactors,[3] energy storage,[4] and so on. Carbonaceous materials from templates of amphiphilic triblock copolymers can form ordered mesostructures with high surface areas and narrow pore-size distributions. The key to the successful generation of mesoporous carbonaceous materials is to utilize organic–organic self-assembly with appropriate block copolymers to construct the mesostructure.[5,6]

Recently, a series of mesoporous polymers and carbon materials with different symmetries have been prepared by using a variety of amphiphilic triblock polymers as templates.[7] As opposed to the large number of available surfactants, only a fraction of these amphiphilic triblock copolymers can be utilized to produce highly ordered mesostructures. The most commonly used triblock copolymers are of the type poly(ethylene oxide)-*b*-poly(propylene oxide)-*b*-poly(ethylene oxide) (PEO–PPO–PEO), which are commercially available as pluronics or synperonics. PEO–PPO–PEO triblock copolymers have established morphological behavior, and the interplay between block immiscibility and connectivity generates a rich variety of mesoscopic structures.[8]

[a] Y. Huang, H. Cai, T. Yu, Dr. B. Tu, Prof. Dr. D. Zhao
Department of Chemistry
Shanghai Key Laboratory of Molecular Catalysis and Innovative Materials
Key Laboratory of Molecular Engineering of Polymers
Advanced Materials Laboratory
Fudan University
Shanghai 200433 (China)
Fax: (+86) 21-65641740
E-mail: dyzhao@fudan.edu.cn

[b] Dr. X. Sun
State Key Laboratory of Organometallic Chemistry
Shanghai Institute of Organic Chemistry, CAS
Shanghai 200032 (China)

Supporting information for this article is available on the WWW under http://www.chemasianj.org or from the author.

Tanaka et al. used resorcinol/formaldehyde as carbon precursors and triblock copolymer F127 ($EO_{106}PO_{70}EO_{106}$) as a template to prepare mesoporous carbon materials with channel structures by direct carbonization.[9] Meanwhile, by using amphiphilic triblock copolymers as a template and a soluble low-molecular-weight polymer of phenol and formaldehyde as a precursor, mesoporous polymer and carbon materials with *P6mm* and *Im*$\bar{3}$*m* symmetries were synthesized by Meng et al.[10,11] Bicontinuous *Ia*$\bar{3}$*d* carbonaceous mesostructures can also be obtained by using triblock copolymer P123 ($EO_{20}PO_{70}EO_{20}$) as a template.[12,13] Liang and Dai employed phloroglucinol/formaldehyde as a carbon source, with enhanced hydrogen-bonding interactions of the triblock copolymer F127 template, to form 2D hexagonal mesoporous carbon materials with different morphologies.[14]

In contrast, the reverse triblock copolymers PPO–PEO–PPO are rarely used in the synthesis of ordered mesoporous materials,[15] because of the difficulty of formation of oil-in-water micelles.[16–18] The hydrophobic PPO blocks of PPO–PEO–PPO are present at both ends, and their hydrophobic effect is significant; this enables the copolymers to form a hard micelle, thus resulting in the characteristic phases that occur in the inverse system PEO–PPO–PEO.[19–21] Very recently, we intentionally used a reverse PPO–PEO–PPO triblock copolymer with a long PEO segment in the synthesis of ordered mesoporous polymer and carbon materials, which extended the category of templates available.[22]

Template synthesis from a mixed-surfactant system has been proven to be a versatile and efficient approach to achieve highly ordered mesoporous materials with different symmetries. Charged mixed-surfactant systems, which include cationic–cationic[23,24] and cationic–anionic[25] mixed-surfactant systems, have already been utilized to synthesize ordered mesoporous silicates. Moreover, surfactant systems that involve the triblock copolymer PEO–PPO–PEO, by associating with ionic surfactants,[26] diblock copolymers,[27] or triblock copolymers PEO–PPO–PEO with variable chain length,[28] can also work well in the generation of ordered mesostructured silicates. However, there is no report about the synthesis of ordered mesostructures by using mixed amphiphilic triblock copolymers PEO–PPO–PEO and reverse PPO–PEO–PPO as templates.

Herein, we demonstrate a synthesis of ordered mesostructured carbonaceous materials by using mixed PEO–PPO–PEO and reverse PPO–PEO–PPO triblock copolymers as templates. A series of highly ordered mesoporous polymers and carbon materials with 2D hexagonal *P6mm* and cubic *Fd*$\bar{3}$*m*, *Im*$\bar{3}$*m*, and *Ia*$\bar{3}$*d* structures were achieved by simply adjusting the ratios of F127, reverse $PO_{53}EO_{136}PO_{53}$ (designated R1), and phenolic resol precursors through a solvent-evaporation-induced self-assembly (EISA) process.[11,29] The mixed-block-copolymer system can interact with resols and tend to self-assemble into micellar structures, which provide a suitable template for constructing mesostructures. Synergy effects provide the mixed-triblock-copolymer system with abundant phase behavior.

Highly ordered mesoporous carbonaceous materials of various symmetries were prepared by using phenolic resol as a precursor and mixed triblock copolymers F127–R1 as a template through the solvent EISA method. Pyrolysis above 350 °C under nitrogen atmosphere removed the templates, and further calcination above 600 °C resulted in the corresponding mesoporous carbonaceous frameworks. In the experiments, all the samples were calcined at 600 °C under N_2 for convenience of comparison.

Results and Discussion

Face-Centered *Fd*$\bar{3}$*m* Mesostructure

Ordered mesoporous carbonaceous materials with face-centered cubic structures (space group *Fd*$\bar{3}$*m*) can only be synthesized in the reverse-triblock-copolymer (R1) system with a copolymer/phenol/formaldehyde molar ratio of 0.0065:1:2, and addition of a small amount of F127 can influence the

Abstract in Chinese:

以 resol 型低聚酚醛树脂为前驱体，混合三嵌段共聚物 PEO-PPO-PEO（F127）和反相 PPO-PEO-PPO 为模板，通过溶剂挥发自组装法，成功地合成出一系列具有不同对称性的、高度有序的介孔碳材料。X-射线散射（SAXS）、电子透射显微（TEM）以及氮气吸附测试结果表明，简单变化嵌段共聚物与 resol 前驱体的比例以及 F127 的相对含量，可以方便地调节介孔碳的结构，可以实现从面心立方相（*Fd*$\bar{3}$*m*）到体心立方相（*Im*$\bar{3}$*m*），甚至到二维六方相（*P6mm*），最终到双连续立方相（*Ia*$\bar{3}$*d*）的相转变。Resol 前驱体可以与由正、反三嵌段共聚物相互交联形成的胶束发生氢键作用，通过有机－有机自组装形成有序介观结构。600 °C 焙烧所得到的介孔碳材料的 BET 比表面积约为 600 $m^2 g^{-1}$，孔径大小在 2.8 到 5.4 nm 范围内可调。对正、反相混合嵌段共聚物在有机－有机自组装过程中行为的理解为结构可控的新型介孔材料的合成研究提供了新的思路。

mesophase. The small-angle X-ray scattering (SAXS) pattern of the as-synthesized sample S1 shows six poorly resolved peaks (Figure 1a). After calcination at 600 °C under nitrogen, the SAXS pattern of the sample became more resolved, and eight diffraction peaks were observed. The q-value ratios of these peaks are $\sqrt{3}:\sqrt{8}:\sqrt{11}:\sqrt{19}:\sqrt{27}:\sqrt{36}:\sqrt{56}:\sqrt{76}$, which were carefully indexed as the 111, 220, 311, 331, 333 (511), 442 (and/or 600), 642, and 662 reflections of the face-centered cubic mesostructure with space group $Fd\bar{3}m$. The lattice parameters for the as-synthesized and calcined samples were calculated[11,22] to be 45.1 and 32.6 nm, respectively, thus suggesting a framework shrinkage of 27.7%. This indicates that the framework undergoes a further condensation process during calcination. The representative TEM images and corresponding Fourier diffractograms (Figure 2a and b) show that the sample S1 contains a high degree of periodicity over large domains, viewed from the [110] and [211] directions. The observable reflections from the Fourier diffractograms and the SAXS data can be summarized as $\{hkl: h+k, h+l, k+l=2n\}$, $\{0kl: k+l=4n\}$, and $\{h00: h=4n\}$, which further confirms that the mesostructure has highly ordered face-centered cubic ($Fd\bar{3}m$) symmetry. The 600 reflection is forbidden for the $Fd\bar{3}m$ mesostructure. Therefore, it can be removed from the SAXS patterns. The lattice parameter estimated from TEM images is approximately 31.9 nm, which is consistent with that determined from the SAXS data.

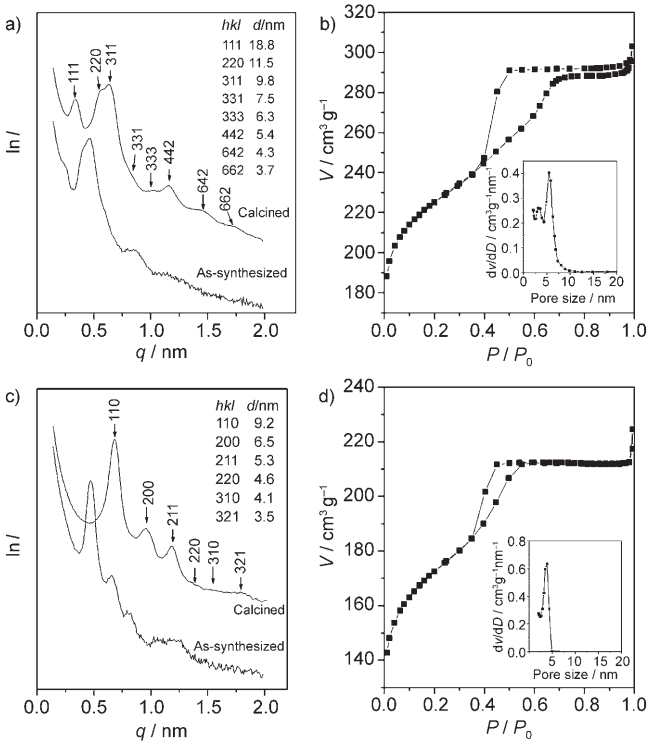

Figure 1. a) SAXS pattern and b) nitrogen-sorption isotherm (inset: pore-size distribution) for the face-centered cubic $Fd\bar{3}m$ mesoporous carbon sample (S1). c) SAXS pattern and d) nitrogen-sorption isotherm (inset: pore-size distribution) for the body-centered cubic $Im\bar{3}m$ mesoporous carbon sample (S2).

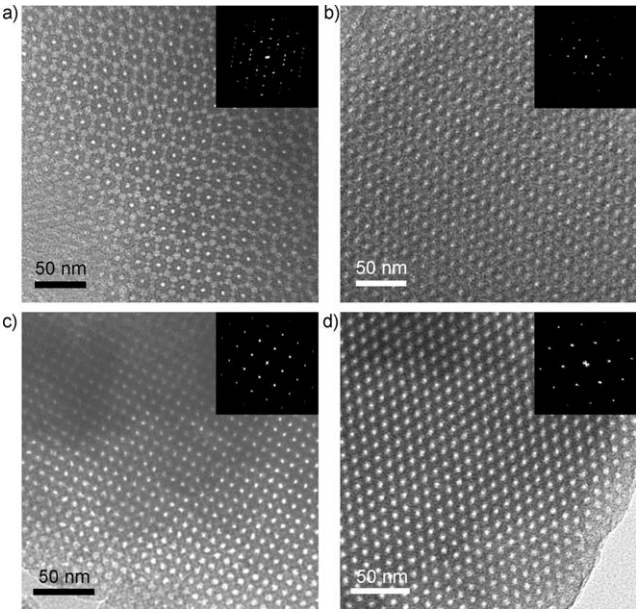

Figure 2. TEM images (inset: Fourier diffractograms) taken along the a) [110] and b) [211] directions of the face-centered cubic $Fd\bar{3}m$ mesoporous carbon sample (S1), and along the c) [100] and d) [111] directions of the body-centered cubic $Im\bar{3}m$ mesoporous carbon sample (S2).

The nitrogen adsorption–desorption isotherms (Figure 1b) of the calcined sample S1 exhibit typical type-IV curves with an H_2-type hysteresis loop, thus implying the caged mesopores with small windows. Notably, a broad capillary condensation characteristic with two clear rapidly increasing steps was observed in the adsorption branch at a relative pressure (P/P_0) of 0.4–0.7. Bimodal pore-size distributions were clearly observed (Figure 1b, inset), which suggests that the carbonaceous sample (S1) has two types of caged mesopores related to the face-centered cubic $Fd\bar{3}m$ mesostructure.[30,31] The calculated pore size of the small cages is 3.2 nm and that of large cages is 5.4 nm. The Brunauer–Emmett–Teller (BET) surface area of calcined sample S1 is 590 $m^2 g^{-1}$, and the pore volume is 0.35 $cm^3 g^{-1}$ (Table 1).

Body-Centered $Im\bar{3}m$ mesostructure

A mesophase transformation occurred with an increase in the amount of triblock copolymer F127 in the organic–organic self-assembly. The SAXS pattern (Figure 1c) of the as-synthesized sample S2 shows six resolved diffraction peaks with q values of 0.469, 0.661, 0.812, 0.938, 1.048, and 1.241 nm^{-1}. After calcination at 600 °C under N_2, the diffraction peaks became more resolved and shifted to higher q values with ratios of $1:\sqrt{2}:\sqrt{3}:\sqrt{4}:\sqrt{5}:\sqrt{7}$. Taken with the TEM observations (see below), these diffractions were indexed as the 110, 200, 211, 220, 310, and 321 reflections of the body-centered cubic mesostructure with space group $Im\bar{3}m$. The lattice parameters were calculated for the as-synthesized and calcined samples S2 to be 18.9 and 13.0 nm, re-

Table 1. Physicochemical properties of mesoporous carbonaceous materials with different symmetries (calcined at 600 °C in N_2) prepared with a mixture of triblock copolymers as templates by the EISA method.

Samples Copolymers/phenol/formaldehyde	R1/F127	Mesostructure	Cell parameter [nm]	BET surface area [m^2g^{-1}]	Micropore area [m^2g^{-1}]	Pore size [nm]	Pore volume [cm^3g^{-1}]
0.0065:1:2	∞	$Fd\bar{3}m$	32.6	590	400	3.2, 5.4	0.35
	2:1	$Im\bar{3}m$	13.4	600	400	3.7	0.35
	1:1	$Im\bar{3}m$	13.0	600	390	3.7	0.37
	1:2	$Im\bar{3}m$	12.9	590	390	3.7	0.39
	0	$Im\bar{3}m$	12.7	580	400	3.8	0.36
0.013:1:2	∞	*P6mm*[a]	11.2	650	380	3.4	0.38
	2:1	*P6mm*[a]	10.5	630	350	3.3	0.39
	1:1	*P6mm*	9.6	600	310	3.3	0.37
	1:2	*P6mm*	9.7	600	310	3.2	0.38
	0	*P6mm*	9.2	590	330	3.0	0.32
0.016:1:2	4:1	$Ia\bar{3}d$	21.8	620	370	2.8	0.33

[a] Contains a little of the $Ia\bar{3}d$ mesophase.

spectively. The framework shrinkage was about 31.2%, which is a little bit larger than that for sample S1. The TEM images viewed along the [100] and [111] directions together with the corresponding Fourier diffractograms (Figure 2c and d) further reveal that the carbonaceous product (S2) has a highly ordered arrangement of mesopores with a body-centered cubic ($Im\bar{3}m$) structure.

The nitrogen adsorption–desorption isotherms of the calcined sample S2 also exhibit typical type-IV curves with an H_2-type hysteresis loop, which corresponds to a 3D caged mesostructure (Figure 1d). Unlike the bimodal pore system of the $Fd\bar{3}m$ mesostructure, the nitrogen sorption measurements of the body-centered cubic $Im\bar{3}m$ mesostructured carbonaceous S2 reveal a uniform pore-size distribution centered at 3.7 nm (Table 1). The BET surface area and the pore volume were calculated to be 600 m^2g^{-1} and 0.37 cm^3g^{-1}, respectively.

In the case of the R1–F127 mixed-surfactant system as the template, when the copolymer (R1-F127)/phenol/formaldehyde molar ratio was fixed at 0.0065:1:2, the body-centered cubic ($Im\bar{3}m$) mesostructure was obtained over a wide range (2–0) of R1/F127 ratios (Figure 3a). The SAXS patterns

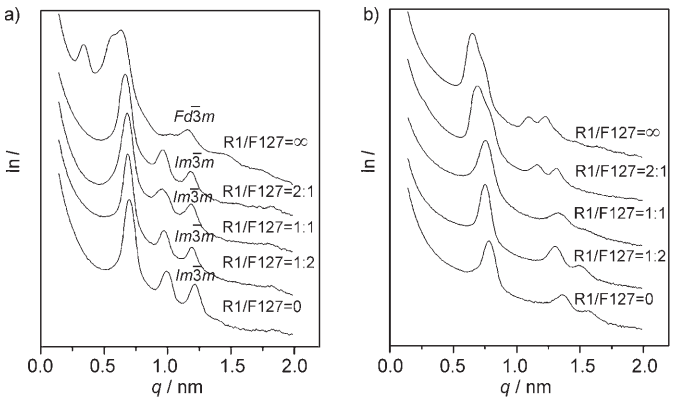

Figure 3. SAXS patterns of the calcined mesoporous carbon materials synthesized by using a template of the mixed-triblock-copolymer surfactant system with the copolymer/phenol/formaldehyde molar ratio fixed at a) 0.0065:1:2 and b) 0.013:1:2 while changing the ratio of R1/F127.

show that the 311 reflection peak at a q value of 0.65 nm^{-1} for the $Fd\bar{3}m$ mesostructure changed to the 110 reflection for the $Im\bar{3}m$ mesostructure, due to changes in the spatial arrangement of the pores and lattice parameters. The q value for the 110 reflection of the $Im\bar{3}m$ mesostructure slightly increased with an increase in the amount of F127 in the mixed-surfactant system. However, the BET surface areas, pore sizes, and pore volumes of the resulting samples were independent of the amount of F127 (Table 1).

2D Hexagonal *P6mm* Mesostructure

A mesophase transformation from the body-centered cubic ($Im\bar{3}m$) to the 2D hexagonal (*P6mm*) mesostructure occurred when the surfactant/phenol/formaldehyde ratio was changed to 0.013:1:2. The SAXS pattern (Figure 4a) of the as-synthesized sample S3 displays the three typical diffraction peaks for 2D hexagonal symmetry. After calcination at 600 °C, three resolved peaks indexed as the 10, 11, and 20 reflections of hexagonal *P6mm* symmetry were observed, which suggests that the mesostructure is stable. The calculated lattice parameters are 15.9 and 9.6 nm for the as-synthesized and calcined sample S3, respectively, thus suggesting a large structural shrinkage of 39.6%. The typical stripelike and hexagonally arranged structures in the TEM images (Figure 5a and b) recorded along the [001] and [110] directions, respectively, were observed, which further confirms a high-quality *P6mm* hexagonal mesostructure. The unit lattice parameter of calcined sample S3 estimated from the TEM images is 9.6 nm, which is in a good agreement with the value calculated from the SAXS data.

The N_2 sorption isotherms of the S3 sample calcined at 600 °C in nitrogen show typical type-IV curves with a clear condensation step at $P/P_0 = 0.4$–0.6 (Figure 4b), thus indicating a uniform mesopore-size distribution. A peculiar hysteresis loop between the H_1 and H_2 type was observed, which might be caused by an intermediate pore structure between cagelike and cylindrical from the phase transformation.[32] The sample exhibited a pore size of 3.3 nm, a BET surface area of 600 m^2g^{-1}, and a pore volume of 0.37 cm^3g^{-1}.

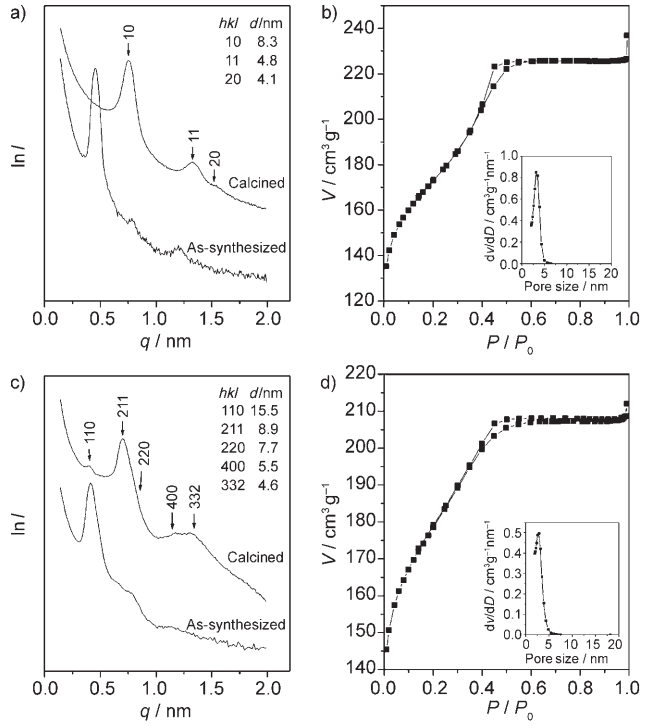

Figure 4. a) SAXS pattern and b) nitrogen-sorption isotherm (inset: pore-size distribution) for the 2D hexagonal *P6mm* mesoporous carbon sample (S3). c) SAXS pattern and d) nitrogen-sorption isotherm (inset: pore-size distribution) for the bicontinuous cubic $Ia\bar{3}d$ mesoporous carbon sample (S4).

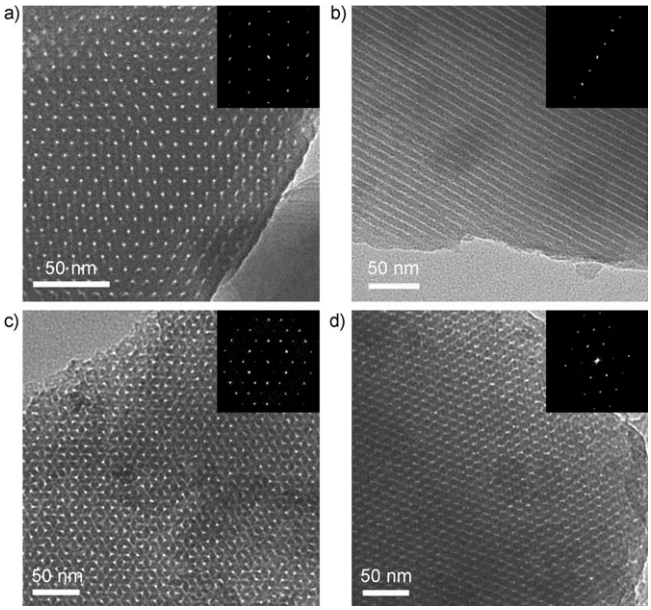

Figure 5. TEM images (inset: Fourier diffractograms) taken along the a) [001] and b) [110] directions of the 2D hexagonal *P6mm* mesoporous carbon sample (S3), and along the c) [111] and d) [311] directions of the bicontinuous cubic $Ia\bar{3}d$ mesoporous carbon sample (S4).

When the amount of R1 exceeded that of F127 (R1/F127 > 1) and the copolymer/phenol/formaldehyde ratio was fixed at 0.013:1:2, the SAXS patterns (Figure 3b) of the resulting materials show a shoulder on the first intense diffraction peak. The ratio of the *d* values calculated from the SAXS data is somehow close to that (d_{211}/d_{220}) for bicontinuous cubic $Ia\bar{3}d$ symmetry. However, the TEM measurements show a 2D hexagonal mesostructure over a large periodic ordered domain (see Supporting Information, Figure S1). This phenomenon may be attributed to a distorted *P6mm* mesostructure that is slightly mixed with a cubic $Ia\bar{3}d$ mesophase. With a decrease in the R1/F127 ratio, the SAXS patterns show good 2D hexagonal mesostructures, and the *q* value of the 10 reflection increased, which corresponds to a small lattice parameter. The BET surface areas, pore sizes, and pore volumes of the hexagonal mesostructured samples decreased slightly (Table 1).

Bicontinuous $Ia\bar{3}d$ Mesostructure

Another mesophase with the bicontinuous cubic $Ia\bar{3}d$ structure was obtained by simultaneously increasing the amount of phenolic resol precursor, while keeping the R1/F127 ratio higher than 4:1. The SAXS pattern (Figure 4c) of the as-synthesized sample S4 shows one intense diffraction peak at a *q* value of 0.41 nm^{-1} and other weak peaks at *q* values of 0.65–1.25. After calcination at 600 °C under nitrogen, four resolved diffraction peaks were observed, which were indexed as the 211, 220, 420, and 332 reflections of cubic $Ia\bar{3}d$ symmetry; this suggests a highly ordered mesostructure. A weak diffraction peak indexed as the 110 reflection was also observed in the SAXS pattern of calcined sample S4, which suggests a small structural defect of $I4_132$ symmetry.[13,33] The calculated lattice parameters are 37.4 and 21.8 nm for the as-synthesized and calcined samples, respectively. The characteristic TEM images (Figure 5c and d) along the [111] and [311] directions provide further evidence for the formation of the bicontinuous cubic $Ia\bar{3}d$ mesostructure. The planar defects and structural distortion were also observed in the TEM images viewed along the [111] direction, which may be caused by the inhomogeneous shrinkage of the mesostructure during calcination.

The nitrogen sorption isotherms (Figure 4d) illustrate that calcined sample S4 has typical type-IV curves with a clear capillary-condensation step, thus suggesting the presence of a uniform mesopore. A narrow pore-size distribution with a mean value of 2.8 nm was calculated from the Barrett–Joyner–Halenda (BJH) model. Notably, the bicontinuous cubic $Ia\bar{3}d$ mesostructure was only formed in a very narrow R1/F127 range. If the amount of F127 exceeds that of R1 by 25% in the mixed amphiphilic surfactant system, a less ordered mesostructure tends to form.

Self-Assembly of Mixed Triblock Copolymers

The micellization process of block copolymers has some inherent complexity due to their structural characteristics such as block length, composition, and architecture. There have been many studies on the self-assembly process and mesophase formation from PEO–PPO–PEO-type copolymer

CHEMISTRY
AN ASIAN JOURNAL

templates.[34–36] In contrast, reverse-type PPO–PEO–PPO copolymers are seldom used to synthesize mesoporous materials, because it is thermodynamically difficult to form mesostructures under general hydrophilic synthesis conditions. The sequence of PPO and PEO segments can greatly influence the physicochemical behavior of the copolymers in the micellization process. During the EISA process, when the concentration of PPO–PEO–PPO in the system reaches the critical micelle concentration (CMC), three possible configurations for reverse PPO–PEO–PPO may be formed (Figure 6a).[37,38] The dangling configuration would lead to one hydrophobic PPO segment highly exposed to the hydrophilic matrix, which is energetically unfavorable. The loop configuration is that of micelle formation, which is quite similar to the configuration of the PEO–PPO–PEO copolymers. However, it has an entropic penalty from the intense folding of the PEO segments. The reverse PPO–PEO–PPO copolymer with a long PEO chain is therefore deliberately used to lower the curving energy and to form the mesophase with high curvature. The configuration that is most clearly different from the micelles of PEO–PPO–PEO is the bridging configuration, in which the two outer PPO blocks participate in two different micelles or aggregates. This behavior leads to an interconnected micelle network for reverse PPO–PEO–PPO.

The interplay of PPO–PEO–PPO and PEO–PPO–PEO between block immiscibility and connectivity generates a rich variety of mesoscopic structures. In the case of the individual reverse PPO–PEO–PPO (R1) with a long PEO chain as a template, it can be deduced that two sets of intercrossing micelles of different sizes can be formed, which is closely related to its specific folding behavior.[18,39,40] This results in the formation of a unique bimodal pore mesostructure with face-centered cubic ($Fd\bar{3}m$) symmetry. It is well-known that increasing the hydrophilic/hydrophobic ratio leads to a mesophase with a higher interface curvature. In the case of a fixed copolymer/precursor ratio, the hydrophilic/hydrophobic effect is largely determined by the PEO/PPO ratio. As the PEO/PPO ratio of F127 is much larger than that of R1, the hydrophilic/hydrophobic ratio of the copolymer system is increased with the addition of F127. The mesostructure changes from $Fd\bar{3}m$ to $Im\bar{3}m$, which has a lower interface curvature, thus indicating that the special comicellization behavior and connectivity also play important roles in the phase transformation. This suggests that the F127 molecules are incorporated into the uniform cross-linked micelle networks,[40,41] which tend to make their size uniform. In the mixed-triblock-copolymer system, the hydrophobic PPO segments are buried inside, away from contact with the hydrophilic matrix; most of the hydrophilic PEO segments have a strong affinity with the resol precursors and self-organize through hydrogen-bonding interactions into spherical or cylindrical domains or gyroid interpenetrating networks (Figure 6b). A sequence of mesostructures, from the 3D mesocage structure ($Fd\bar{3}m$ and $Im\bar{3}m$) to the 2D hexagonal ($P6mm$) and then the 3D bicontinuous mesostructure ($Ia\bar{3}d$), was derived with a decrease in the R1/F127 ratio and/or the copolymer/resol precursor ratio. Due to the strong affinity between resol and the hydrophilic PEO blocks, the increase in the amount of resol can lead to an expansion of the hydrophilic domain in the composite micelles, thus resulting in an increase in interface curvature (Figure 6c).[10,26] In this way, the mesostructure changes from that of high curvature to that of low curvature.

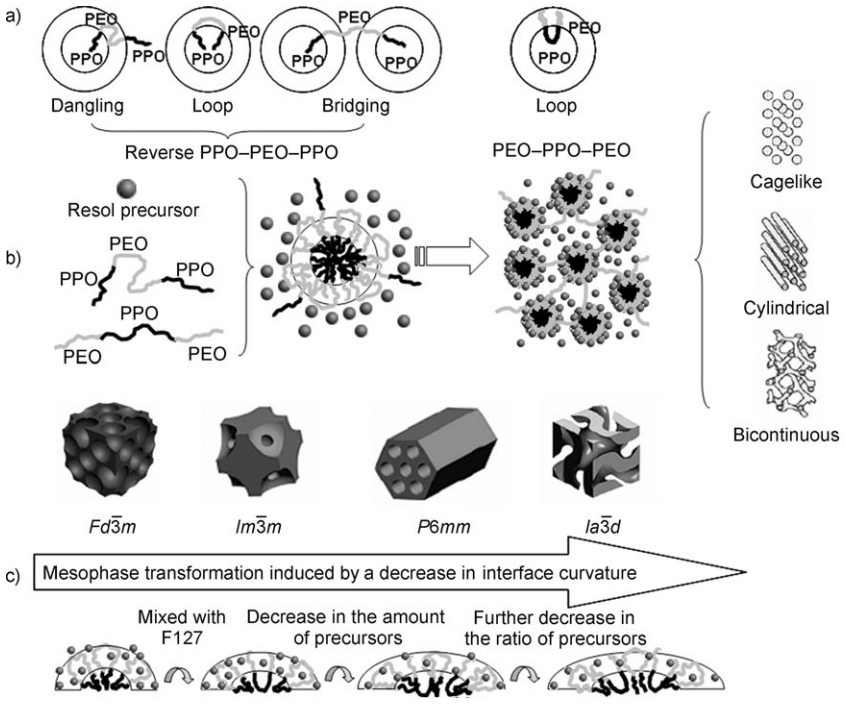

Figure 6. Schematic representation of the possible configurations of PEO–PPO–PEO and reverse PPO–PEO–PPO triblock copolymers during a) the EISA process, b) the formation of mixed-type cross-linking micelles and self-assembly, and c) mesophase transformation induced by a decrease of the interface curvature. With comicellization of PEO–PPO–PEO and PPO–PEO–PPO and a decrease in the amount of resol precursors, the interface curvature of mixed amphiphilic micelles was decreased, thus resulting in the mesophase transformation from cubic close-packing to loose packing.

Conclusions

We have demonstrated a successful synthesis of highly ordered mesoporous carbonaceous frameworks with variable cubic $Fd\bar{3}m$, $Im\bar{3}m$, $Ia\bar{3}d$, and hexagonal symmetries by

using mixed amphiphilic surfactants of reverse triblock copolymer R1 ($PO_{53}EO_{136}PO_{53}$) and F127 ($EO_{106}PO_{70}EO_{106}$) as the template and phenolic resol as the carbon precursor through the EISA strategy. The ordered mesoporous carbonaceous material with face-centered cubic $Fd\bar{3}m$ symmetry, in particular, shows a bimodal pore system with mean pore diameters of 3.2 and 5.4 nm and a small window size, which is associated with the characteristic phase behavior of reverse triblock copolymers PPO–PEO–PPO. The carbonaceous mesostructures can be transformed from high curvature to low ($Fd\bar{3}m \rightarrow Im\bar{3}m \rightarrow P6mm \rightarrow Ia\bar{3}d$) by simply adjusting the R1/F127 and copolymer/resol precursor ratios. The PEO–PPO–PEO-type and PPO–PEO–PPO-type triblock copolymers can interplay and simultaneously contribute to the micellization process and organic–organic self-assembly through hydrogen-bonding interactions to form intercrossing micelle networks. The use of mixed amphiphilic copolymers of PEO–PPO–PEO and PPO–PEO–PPO could have wide-ranging applicability for the development of new mesoporous materials.

Experimental Section

Chemicals

Triblock PEO–PPO–PEO copolymer pluronic F127 ($EO_{106}PO_{70}EO_{106}$) was purchased from Acros Corp. Reverse triblock copolymer R1 ($PO_{53}EO_{136}PO_{53}$) was prepared from an anionic-polymerization method by using KOH as a catalyst. In a typical preparation, poly(ethylene glycol) 6000 (PEG 6000; 5.0 g) and propylene oxide (PO; 12 mL) monomer were mixed in an autoclave at ambient temperature. KOH (0.10 g) was then added, and the mixture was heated at 120 °C under nitrogen for 24 h. After cooling to room temperature, the catalyst was neutralized by adding acetic acid and then removed by centrifugation. The polymer was dissolved in toluene. The final product (13.6 g, 90.8 % yield) was collected by recrystallization from isooctane, with an M_n of 12000 and the molar EO/PO-segment ratio of 1.28 determined by ^{1}H NMR spectroscopy (see Supportin Information, Figure S2). As the molecular weight of block copolymers F127 and R1 used for the experiments were only slightly different, we used the mean value of 12000 as their molecular weight for convenience. Other chemicals were purchased from Shanghai Chemical Corp. All chemicals were used as received without further purification. Millipore water was used in all experiments.

Syntheses

Phenolic resol precursor: Soluble phenolic resols were prepared under basic conditions according to the previously reported procedure.[11] Phenol (1.0 g, 10.6 mmol) was melted at 50 °C, then a solution of NaOH (20 wt %, 0.21 g, 1.06 mmol) was added with stirring over 10 min. After formalin (37 wt %, 1.725 g, 21.2 mmol) was added dropwise, the mixture was stirred at 75 °C for 1 h and cooled to room temperature. A solution of HCl (0.6 M) was used to adjust the pH of the mixture to neutral, after which water was removed. The obtained phenolic resol ($M_n < 500$ measured by gel-permeation chromatography (GPC)) was redissolved in ethanol for further use.

Face-centered cubic ($Fd\bar{3}m$) S1: S1 was synthesized by using triblock copolymers as a template and phenolic resols as a precursor with a copolymer/phenol/formaldehyde molar ratio of 0.0065:1:2, with R1/F127 = ∞. In a typical synthesis, R1 (0.30 g) was dissolved in ethanol (5.0 g). The resol precursor (5.0 g) containing phenol (0.36 g, 3.8 mmol) and formaldehyde (0.23 g, 7.6 mmol) was then added with stirring over 10 min to form a homogeneous solution. A transparent film was obtained by pouring the solution into dishes to evaporate the ethanol at room temperature for 6 h and further heating in an oven at 100 °C for 24 h. The as-synthesized products were collected and calcined at 600 °C for 4 h at a heating rate of 1 °C min^{-1} under nitrogen atmosphere to obtain the final product S1.

Body-centered cubic ($Im\bar{3}m$) S2: S2 was prepared by using mixed triblock copolymers as templates with a copolymer/phenol/formaldehyde molar ratio of 0.0065:1:2, with R1/F127 = 1:1. In a typical synthesis, R1 (0.15 g) and F127 (0.15 g) were dissolved in ethanol (5.0 g). The resol precursor (5.0 g) containing phenol (0.36 g, 3.8 mmol) and formaldehyde (0.23 g, 7.6 mmol) was then added with stirring over 10 min to form a homogeneous solution. The subsequent thermopolymerization and calcination process were performed according to the above procedure.

Two-dimensional hexagonal (*P6mm*) S3: S3 was prepared by using mixed triblock copolymers as templates with a copolymer/phenol/formaldehyde molar ratio of 0.013:1:2, with R1/F127 = 1:1. In a typical synthesis, R1 (0.15 g) and F127 (0.15 g) were dissolved in ethanol (5.0 g). The resol precursor (5.0 g) containing phenol (0.18 g, 1.9 mmol) and formaldehyde (0.12 g, 3.8 mmol) was then added with stirring over 10 min to form a homogeneous solution. The subsequent thermopolymerization and calcination process were performed according to the above procedure.

Bicontinuous cubic ($Ia\bar{3}d$) S4: S4 was prepared by using mixed triblock copolymers as templates with a copolymer/phenol/formaldehyde molar ratio of 0.016:1:2, with R1/F127 = 4:1. In a typical synthesis, R1 (0.24 g) and F127 (0.06 g) were dissolved in ethanol (5.0 g). The resol precursor (5.0 g) containing phenol (0.15 g, 1.6 mmol) and formaldehyde (0.10 g, 3.3 mmol) was then added with stirring over 10 min to form a homogeneous solution. The subsequent thermopolymerization and calcination process were performed according to the above procedure.

Characterization

SAXS measurements were taken on a Nanostar U SAXS system with $Cu_{K\alpha}$ radiation (40 kV, 35 mA). Nitrogen adsorption–desorption isotherms were recorded at 77 K with a Micrometritics Tristar 3000 analyzer. Before the analysis, the samples were degassed in vacuum at 200 °C for at least 6 h. The BET method was utilized to calculate the specific surface areas and the pore volume, and pore-size distributions were derived from the adsorption branches of the isotherms by the BJH model. TEM images were obtained with a JEOL 2011 microscope operating at 200 kV. The samples for TEM measurements were suspended in ethanol and supported on a holey-carbon film on a Cu grid.

Acknowledgements

We thank Prof. Dr. Y. Tang of the Shanghai Institute of Organic Chemistry, CAS, for helpful suggestions and discussion for the preparation of the copolymers. This work was supported by the NSF of China (20421303 and 20521140450), the State Key Basic Research Program of the PRC (2006CB202502 and 2006CB0N0302), Shanghai Nanotech Promotion Center (0652nm024), the Shanghai Education Committee (02SG01), the Program for New Century Excellent Talents in University (NCET-04–03), and the Shanghai Science and Technology Committee (06DJ14006, 055207078, and 05DZ22313).

[1] S. H. Joo, S. J. Choi, I. Oh, J. Kwak, Z. Liu, O. Terasaki, R. Ryoo, *Nature* **2001**, *412*, 169–172.
[2] D. Lee, J. Lee, J. Kim, J. Kim, H. B. Na, B. Kim, C. H. Shin, J. H. Kwak, A. Dohnalkova, J. W. Grate, T. Hyeon, H. S. Kim, *Adv. Mater.* **2005**, *17*, 2828–2833.
[3] M. Hartmann, *Chem. Mater.* **2005**, *17*, 4577–4593.
[4] H. S. Zhou, S. M. Zhu, M. Hibino, I. Honma, M. Ichihara, *Adv. Mater.* **2003**, *15*, 2107–2111.
[5] Y. Wan, Y. F. Shi, D. Y. Zhao, *Chem. Commun.* **2007**, 897–926.
[6] Y. Wan, H. F. Yang, D. Y. Zhao, *Acc. Chem. Res.* **2006**, *39*, 423–432.
[7] J. Lee, J. Kim, T. Hyeon, *Adv. Mater.* **2006**, *18*, 2073–2094.
[8] B. Smarsly, M. Antonietti, *Eur. J. Inorg. Chem.* **2006**, *6*, 1111–1119.

[9] S. Tanaka, N. Nishiyama, Y. Egashira, K. Ueyama, *Chem. Commun.* **2005**, 2125–2127.
[10] Y. Meng, D. Gu, F. Zhang, Y. F. Shi, L. Cheng, D. Feng, Z. X. Wu, Z. X. Chen, Y. Wan, A. Stein, D. Y. Zhao, *Chem. Mater.* **2006**, *18*, 4447–4464.
[11] Y. Meng, D. Gu, F. Q. Zhang, Y. F. Shi, H. F. Yang, Z. Li, C. Z. Yu, B. Tu, D. Y. Zhao, *Angew. Chem.* **2005**, *117*, 7215–7221; *Angew. Chem. Int. Ed.* **2005**; *44*, 7053–7059.
[12] F. Q. Zhang, Y. Meng, D. Gu, Y. Yan, Z. X. Chen, B. Tu, D. Y. Zhao, *Chem. Mater.* **2006**, *18*, 5279–5288.
[13] F. Q. Zhang, Y. Meng, D. Gu, Y. Yan, C. Z. Yu, B. Tu, D. Y. Zhao, *J. Am. Chem. Soc.* **2005**, *127*, 13508–13509.
[14] C. D. Liang, S. Dai, *J. Am. Chem. Soc.* **2006**, *128*, 5316–5317.
[15] L. H. Pei, K. Kurumada, M. Tanigaki, M. Hiro, K. Susa, *J. Colloid Interface Sci.* **2005**, *284*, 222–227.
[16] P. Alexandridis, U. Olsson, B. Lindman, *J. Phys. Chem.* **1996**, *100*, 280–288.
[17] R. Jiang, Q. H. Jin, B. H. Li, D. T. Ding, A. C. Shi, *Macromolecules* **2006**, *39*, 5891–5896.
[18] K. Mortensen, *Macromolecules* **1997**, *30*, 503–507.
[19] P. Alexandridis, U. Olsson, B. Lindman, *Langmuir* **1996**, *12*, 1419–1422.
[20] P. Alexandridis, U. Olsson, B. Lindman, *Langmuir* **1998**, *14*, 2627–2638.
[21] H. Delacroix, T. Gulik-Krzywicki, J. M. Seddon, *J. Mol. Biol.* **1996**, *258*, 88–103.
[22] Y. Huang, H. Q. Cai, T. Yu, F. Q. Zhang, F. Zhang, Y. Meng, D. Gu, Y. Wan, X. L. Sun, B. Tu, D. Y. Zhao, *Angew. Chem.* **2007**, *119*, 1107–1111; *Angew. Chem. Int. Ed.* **2007**, *46*, 1089–1093; .
[23] K. Hou, L. Shen, F. Y. Li, Z. Q. Bian, C. H. Huang, *J. Phys. Chem. B* **2006**, *110*, 9452–9460.
[24] R. Ryoo, C. H. Ko, I. S. Park, *Chem. Commun.* **1999**, 1413–1414.
[25] A. Lind, B. Spliethoff, M. Linden, *Chem. Mater.* **2003**, *15*, 813–818.
[26] D. H. Chen, Z. Li, Y. Wan, X. J. Tu, Y. F. Shi, Z. X. Chen, W. Shen, C. Z. Yu, B. Tu, D. Y. Zhao, *J. Mater. Chem.* **2006**, *16*, 1511–1519.
[27] J. M. Kim, Y. Sakamoto, Y. K. Hwang, Y. U. Kwon, O. Terasaki, S. E. Park, G. D. Stucky, *J. Phys. Chem. B* **2002**, *106*, 2552–2558.
[28] T. W. Kim, R. Ryoo, M. Kruk, K. P. Gierszal, M. Jaroniec, S. Kamiya, O. Terasaki, *J. Phys. Chem. B* **2004**, *108*, 11480–11489.
[29] D. Grosso, F. Cagnol, G. Soler-Illia, E. L. Crepaldi, H. Amenitsch, A. Brunet-Bruneau, A. Bourgeois, C. Sanchez, *Adv. Funct. Mater.* **2004**, *14*, 309–322.
[30] A. E. Garcia-Bennett, K. Miyasaka, O. Terasaki, S. A. Che, *Chem. Mater.* **2004**, *16*, 3597–3605.
[31] A. E. Garcia-Bennett, O. Terasaki, S. A. Che, T. Tatsumi, *Chem. Mater.* **2004**, *16*, 813–821.
[32] F. Kleitz, L. A. Solvyov, G. M. Anilkumar, S. H. Choi, R. Ryoo, *Chem. Commun.* **2004**, 1536–1537.
[33] R. Ryoo, S. H. Joo, S. Jun, *J. Phys. Chem. B* **1999**, *103*, 7743–7746.
[34] P. Kipkemboi, A. Fogden, V. Alfredsson, K. Flodstrom, *Langmuir* **2001**, *17*, 5398–5402.
[35] G. J. A. Sevink, J. G. E. M. Fraaije, H. P. Huinink, *Macromolecules* **2002**, *35*, 1848–1859.
[36] Y. J. Yuan, H. P. Hentze, W. M. Arnold, B. K. Marlow, M. Antonietti, *Nano Lett.* **2002**, *2*, 1359–1361.
[37] C. F. Lin, H. P. Lin, C. Y. Mou, S. T. Liu, *Microporous Mesoporous Mater.* **2006**, *91*, 151–155.
[38] S. H. Kim, W. H. Jo, *J. Chem. Phys.* **2002**, *117*, 8565–8572.
[39] K. Mortensen, W. Brown, E. Jorgensen, *Macromolecules* **1994**, *27*, 5654–5666.
[40] Q. Q. Wang, L. Li, S. P. Jiang, *Langmuir* **2005**, *21*, 9068–9075.
[41] Z. H. Yang, R. Sharma, *Langmuir* **2001**, *17*, 6254–6261.

Received: May 18, 2007
Published online: August 8, 2007

